Sampling effects on the quantification of sodium content in infant formula using laser induced breakdown spectroscopy (LIBS)

Xavier Cama-Moncunill[a, *], Maria Markiewicz-Keszycka[a], Raquel Cama-Moncunill[a], Yash Dixit[a] , Maria P. Casado-Gavalda[a], Patrick J. Cullen[a,b], Carl Sullivan[a]

a) School of Food Science and Environmental Health, Dublin Institute of Technology, Cathal Brugha St, Dublin 1, Ireland

b) Department Chemical and Environmental Engineering, University of Nottingham, UK

*Corresponding author
Xavier Cama-Moncunill
School of Food Science and Environmental Health,
Dublin Institute of Technology, Cathal Brugha St, Dublin 1, Ireland
d14128373@mydit.ie
Tel: +353(0)14024359

Abstract

In the present work, laser-induced breakdown spectroscopy (LIBS) was employed to predict the sodium content of infant formula (IF) over the range of 0.5–4 mg Na/g. Calibration models were built using partial least squares regression (PLS), correlating the LIBS spectral data with reference Na contents quantified by atomic absorption spectroscopy (AAS). The aim of this study was to demonstrate the ability of LIBS as a rapid tool for quantifying sodium in IF, but also to explore strategies concerning the acquisition of measurements with LIBS. A range of different pre-processing techniques, measuring depths (repetition of laser shots) and accumulations were evaluated in terms of PLS performance. The best calibration model was developed using the third-layer spectra normalised by the H I 656.29 nm emission line, yielding a coefficient of determination (R^2) of 0.93, and root-mean-square errors (RMSE) of 0.37 and 0.13 mg/g for cross-validation and validation, respectively.

Industrial relevance

Improving productivity and robustness of manufacturing processes, yet satisfying increasing concerns and strict regulations on the quality and safety of infant products could be achieved through the introduction of optical analytical techniques with real-time capabilities during processing. In this paper, LIBS is proposed as a potential cost-effective screening tool that can provide fast elemental composition analysis of IF. Specifically, the application of LIBS and multivariate data analysis for predicting sodium content over a range in conformity with regulatory guidelines is discussed in this work.

Keywords

LIBS; Infant formula; Sodium; Partial least squares regression; sampling

1. Introduction

Infant formula (IF) is an industrially produced food intended as a substitute for breast milk. IFs are typically based on cow's milk, and followed by several adjustments and addition of ingredients in order to bring the composition closer to that of human milk (Blanchard, Zhu, & Schuck, 2013). Infancy is a crucial period of growth and development, hence IF's composition (e.g. fat, proteins, minerals, etc.) and manufacturing practices are strictly regulated by national authorities to ensure the safety and nutrient profile of infant formula products (Jiang, 2014; Montagne, Van Dael, Skanderby, & Hugelshofer, 2009).

Sodium is an essential mineral; it is the main cation in extracellular fluid playing a vital role in the regulation of osmolarity, acid-base equilibrium, active transport across cells and membrane potential (Guo, 2014). Although a minimum intake is indispensable for healthy functioning, an excessive consumption of sodium in the human diet is related to higher blood pressure and an increased risk of developing cardiovascular diseases (Masotti, Erba, De Noni, & Pellegrino, 2012; Tamm, Bolumar, Bajovic, & Toepfl, 2016). With regard to infancy, studies have also associated an excessive sodium intake with increased blood pressure in the later stages of life, indicating that blood pressure may track with age (Campbell et al., 2014; John et al., 2016).

Conventional well-established methods for mineral analysis in infant formula include atomic absorption spectroscopy (AAS), inductively coupled plasma optical emission spectroscopy (ICP-OES) and inductively coupled plasma mass spectroscopy (ICP-MS) (Poitevin, 2016). These methods, despite their high sensitivity and accuracy, generally require time-consuming and laborious sampling procedures and the use of chemical reagents such as acids and gases, as well as an associated high cost of consumables (e.g. argon) (Wu & Sun, 2013).

Laser-induced breakdown spectroscopy (LIBS) is an analytical technique based on optical emission spectroscopy in which laser pulses are employed as the excitation source to vaporise, atomise and ionise a small part of the target's material. As a result, plasma arising from the sample surface is generated from which photons are released form the excited species in the plasma returning to their ground state levels of energy which can be analysed with spectrometers to infer the elemental composition of the sample (Cremers & Radziemski, 2013). LIBS, yet recent in the area of food analysis, has gained remarkable popularity in the last few years with an increase in the number of publications and extensive reviews concerning food samples (Maria Markiewicz-Keszycka et al., 2017; Sezer, Bilge, & Boyaci, 2017). The advantages that LIBS offers compared to the conventional methods are its speed, a relatively low cost, little to no sample preparation and elemental surface mapping capabilities (Dixit et al., 2017; Kim, Kwak, Choi, & Park, 2012). Further attractive features include: remote sensing, as it constitutes an entirely optical technique, and suitability for on-/at-line applications, altogether allowing the technology to be considered a potential process analytical technology (PAT) for qualitative and quantitative chemical analysis (Cullen, Bakalis, & Sullivan, 2017) (for PAT literature the reader is referred to: Misra et al., 2015; van den Berg et al., 2013). Nonetheless, LIBS also has limitations or drawbacks, especially concerning quantitative analyses. Some of these limitations include signal fluctuations on a shot-to-shot basis (Tognoni & Cristoforetti, 2016) and difficulties in establishing good calibration curves due to strong matrix effects (Ferreira et al., 2010; Lei et al., 2011). Several publications evaluating and discussing strategies with the goal of overcoming such problems can be found in the literature (dos Santos Augusto, Barsanelli, Pereira, & Pereira-Filho, 2017; El Haddad, Canioni, & Bousquet, 2014; Jantzi et al., 2016).

In this study, LIBS and multivariate data analysis with partial least squares regression (PLS) was employed to predict the sodium content of IF samples. In order to provide for reference Na contents, atomic absorption spectroscopy (AAS) was used. The aim of this study was to demonstrate the ability of LIBS as a rapid screening tool for quantifying sodium over a range relevant to IF manufacturing, offering a means for industries to rapidly verify target mineral contents. Furthermore, strategies concerning the acquisition of measurements with LIBS were explored, namely the repetition of laser shots on a single location. Such an approach examines the impact of measuring the inner layers of the sample and, whether to accumulate laser shots or use the spectra collected from a single layer.

2. Material and methods

2.1. Sample preparation

Commercial powdered IF and follow-on formulas (formulas intended for children over 6 months of age) were acquired from a local supermarket in Dublin, Ireland. Lactose (α-lactose monohydrate ≥ 99 %) and sodium chloride (NaCl ≥ 99 %) were purchased from Sigma Aldrich (St. Louis, MO, USA).

Samples with varying content of sodium were prepared by blending IF with sodium chloride or lactose, whether the goal was to increase or decrease the sodium content in the mix. In total, 7 samples were obtained, including one sample which consisted only of IF. The selected range of sodium was approx. from 0.5 to 4 mg/g (concentrations corresponding to the lowest and highest Na content samples, respectively). This range was intended to cover the regulatory sodium levels provided by the Codex Alimentarius Commission (Codex, 2007). Constituents of the mixtures (IF, NaCl and lactose) and follow-on formulas were ground and pre-mixed using a laboratory blender (8011G, Waring Laboratory Science, CT, USA) equipped with rotatory stainless-steel blades for 2 minutes to ensure there were no aggregates occurring in the powders, with the goal of improving subsequent blending performance. Dry mixing was then carried out using a laboratory V-mixer (FTLMV-1L&, Filtra Vibracion S.L., Spain) for 20 minutes. In order to ensure reproducibility, two independent batches were prepared (batch 1 and batch 2). Each batch was composed of the aforementioned 7 samples divided into: 5 calibration samples (referred to as C1–C5), employed for PLS modelling, and 2 validation samples (V1, V2) to test the robustness of the models. In addition to these validation samples, 2 different follow-on formula brand samples (V3, V4) were used to assess the ability of the calibrations for predicting mineral content in infant products with different formulations.

For LIBS analysis, samples were pelletized by pressing approx. 400 mg of each sample using a manual hydraulic press fitted with a 13 mm pellet die (Specac Ltd., UK) at 10 tons for 3 minutes. Pellets were prepared in triplicates (3 replicates per sample), giving a total number of 48 pellets. The two batches of samples were measured on different days.

2.2. Atomic absorption spectroscopy (AAS)

AAS was selected as the reference method for sodium quantification in IF mixtures. Na contents were established using a Varian 55B AA spectrometer (Varian, United States) following the standard method 985.35 for mineral determination in IF of the AOAC (Official Methods of Analysis of AOAC International) with slight modifications. Approximately 1.5 g of each sample was transferred to a crucible in triplicates (3 replicates). Crucibles were placed on a hot plate and heated until smoking ceased. Organic matter was then decomposed by dry ashing in a muffle furnace at 525°C for 4 h. Ashes were dissolved in 50 mL 1 M nitric acid. A further dilution step was required to bring concentrations within the linear range of the instrument (0–1 ppm).

Calibration curves were established by using aqueous standards prepared from a commercial sodium stock solution (Sodium standard for AAS – 1,000 mg/L, Sigma-Aldrich). Sodium absorbance was measured at 589 nm with a slit width of 0.5 nm. All replicates and batches were measured on different days.

2.3. LIBS instrumentation and measurements

2.3.1. Instrument set-up

LIBS spectra were recorded using a LIBSCAN-150 system (Applied Photonics Ltd, UK) described in a previous publication (X. Cama-Moncunill et al., 2017). The system was fitted with a 150 mJ Q-switched Nd:YAG laser (Ultra, Quantel laser, MT, USA) operating at 1064 nm and a pulse duration of 5 ns, coupled to six fibre-optic spectrophotometers (AvaSpec, Avantes spectrometers, Netherlands) covering the wavelength range of 181–904 nm. Moreover, the system was equipped with a miniature CCD camera which enabled the monitoring of the measurements.

For the experiments, plasma emission was analysed with a delay time of 1.27 µs and an integration time of 1.1 ms. The laser was operated with a firing repetition rate of 1 Hz.

2.3.2. Sampling method

Pellets were measured individually using a sample chamber equipped with a three-axis translation stage (Applied Photonics Ltd, UK) which facilitated the acquisition of spectra at multiple locations of the pellet surface, that is, 100 locations following a 10×10 grid pattern. Spectral acquisition was carried out by recording 5 consecutive laser shots (depth measurements) at each of the 100 locations, giving a total number of 500 measurements per pellet. Data resulting from these consecutive laser shots can be considered as spectra corresponding to 5 different layers of the pellets, i.e. the repetitive firing of the laser at the same location causes the ablation of the outer material penetrating and allowing to measure deeper into the sample (Cremers & Radziemski, 2013).

Spectral data collected from the 5 laser shots were stored separately in order to assess the best layer from which to build the sodium quantification model, and to allow subsequent comparison between accumulated and non-accumulated laser shots.

2.4. Data analysis

Data analysis was performed with R (R Core Team, 2014) using the R package “pls” (Mevik, Wehrens, & Liland, 2015) for conducting PLS (partial least squares regression), as well as other in-house functions.

Firstly, the average of the LIBS spectra collected at multiple locations was calculated for each layer, resulting in 5 spectra per pellet. Data was then divided into a training data set (N=30) and a test set (N=12), additionally the follow-on formula extra validation samples (N=6) were tested. Prior to PLS modelling, combinations of different pre-processing techniques and normalisation methods were applied to the spectra with the aim of reducing the signal fluctuations due to extraneous sources of variability and to minimize any matrix effects (Sobron, Wang, & Sobron, 2012). Specifically, the techniques explored were: baseline correction (R package “baseline”), second derivative and standard normal variate (SNV). Spectral normalisation using other approaches, including normalisation by an internal standard and the Euclidean norm, were also explored.

PLS calibration models using the different pre-processing techniques were developed for each of the 5 layers of the pellets. The performance of each model was evaluated by the leave-one-out root-mean-square error of cross-validation (RMSECV) technique, as well as the root-mean-square error of prediction (RMSEP). The wavelength range used for the modelling was limited to 560–825 nm since this region encompassed the main Na emission lines, while decreasing the total number of variables that do not contain useful peaks (Moncayo, Manzoor, Rosales, Anzano, & Caceres, 2017).

In order to provide for a comparison between the accumulated and non-accumulated shots, spectra corresponding to the different layers were summated to one another so that 2, 3, 4 and 5 accumulations were obtained. PLS modelling of the accumulated spectra was then carried out, and their resulting performances were compared to those of the single-layer-spectra models.

The limit of detection was computed according to the pseudounivariate approach (LOD_{pu}) for PLS models as proposed in a publication elsewhere (Allegrini & Olivieri, 2014) in accordance with IUPAC official recommendations. LOD_{pu} calculation was performed as shown in Eq. 1.

$$LOD_{pu} = \frac{3.3}{S_{pu}} \left[\left(1 + h_{0\,min} + \frac{1}{I}\right) var_{pu}\right]^{1/2} \qquad (1)$$

where S_{pu} is the slope of the pseudounivariate line, $h_{o\,min}$ is the minimum leverage when the analyte concentration is zero, I the number of samples employed for calibration, and var_{pu} is the variance of the regression residuals.

3. Results and discussion

3.1. AAS

In AAS, the accuracy of the results relies heavily upon the calibration curve established from reference standard solutions of the desired element. Good calibration curves were obtained rendering values for the coefficient of determination (R^2) ≥ 0.99. Sodium contents of the IF samples determined with AAS, expressed in mg/g, are shown in Table 1.

3.2. LIBS spectral features

An initial exploratory analysis of the LIBS spectra was conducted in order to determine the principal differences among the samples studied. For comparison purposes, the averaged spectra of pellets corresponding to the lactose-IF mixture (C1, approx. 0.5 mg Na/g), pure IF (C2, approx. 1.3 mg Na/g) and the sodium chloride-IF mixture (C5, approx. 3.7 mg Na/g) are shown in Fig. 1. In the figure, several of the most important spectral lines of elements occurring in the spectra can be seen. The main element emission lines in the spectra were identified using the NIST database (Kramida, Ralchenko, Reader, & NIST ASD team, 2016). These emission lines included: C I 247.86 nm, Ca II 393.37; 396.85 nm, Ca I 422.67; 558.88;

612.22; 616.22 nm, H I 656.29 nm, N I 744.23; 746.83 nm, K I 766.49; 769.90 nm, O I 777.19 nm and Na I 589.05; 589.59 nm. Moreover, three Na I lines were identified at 568.26, 568.82 and 819.48 nm. Other possible Na lines in the spectra were discarded and not considered for quantitative analysis since the intensities at these wavelengths were marginal, which is consistent with the NIST guidelines for sodium.

3.3. Multivariate analysis with PLS

PLS is a method for predicting a quantitative response (i.e. sodium content), stored in a matrix Y, from numerous predictor variables (i.e. spectral data), stored in a matrix X. In order to do so, it decomposes simultaneously the two matrices into new variables, known as factors or latent variables (LV), in such a way that they explain as much as possible of the covariance between X and Y. A multivariate linear model is then fitted using the latent variables to predict the quantitative response (Abdi, 2010).

PLS modelling has been demonstrated to successfully develop quantitative calibration models from LIBS spectral data of food samples in previous publications (Andersen, Frydenvang, Henckel, & Rinnan, 2016; Bilge et al., 2016; M. Markiewicz-Keszycka et al., 2018). In the present study, PLS was employed to build the calibration models for the determination of sodium content by correlating the pre-processed LIBS spectra in the wavelength range of 560–825 nm to the reference Na contents extracted from AAS analysis.

3.3.1. PLS modelling: performance of sampling methods and spectral pre-processing

As previously mentioned, different techniques and normalisation methods were explored as pre-processing techniques of the spectra prior to modelling. To this end, various calibrations were developed using the approaches detailed in section 2.4. A summary of PLS performances for these calibrations can be found in Table 2 (for briefness, this table only includes some of the most relevant models). The criterion followed for establishing an optimum number of LVs for each model considered a low value of RMSECV (root-mean-square error of cross-validation) with a low number of LVs to avoid overfitting. In order to determine the best calibration for quantifying sodium content in IF samples, both RMSECV and RMSEP (root-mean-square error of prediction) were used.

With regards to pre-processing techniques, the best performances were obtained for normalised spectra with SNV, Euclidean norm and normalisation using the H I at 656.29 nm and Ca I at 422.6 nm emission lines as internal standards. All the methods above yielded similar results for calibration (Table 2): e.g. the third-layer-spectra models (measurement depth: 3) using these pre-processing techniques rendered values of almost 0.94 for the coefficient of determination (R^2). These models also provided similar results for root-mean-square errors of cross-validation and prediction: third-layer-spectra models yielded values of approx. 0.37 mg/g for RMSECV and values in the range of approx. 0.13–0.16 mg/g for RMSEP. Other techniques such as baseline correction or normalisation with other internal standards (C I at 247.9nm and K I at 766.4 nm) provided good calibrations and reasonable validation performances. However, the RMSEP values were slightly higher than those obtained with SNV, Euclidean, H I 656.29 nm or Ca I 422.6 nm. Second derivative pre-processing was found not to be effective for calibration showing low values of R^2 and R^2_{CV} (coefficient of determination for cross-validation), as well as high values of root-mean-square errors (RMSE, RMSECV).

Regarding the modelling of layers or depth measurements, it was observed that the third-layer spectra exhibited the best results regardless of the pre-processing techniques used. The first and second layers, while providing a good calibration, showed performances considerably lower for cross-validation and validation. The fourth and fifth layers exhibited an overall good performance, but with lower R^2 values and higher RMSECV and RMSEP as compared to the third layer. The effect of measuring deeper into the sample on spectral quality, and as a mechanism to avoid surface contamination has been previously investigated (R. Cama-

Moncunill et al., 2017). Similarly, in this publication PLS models were developed for different layers of the samples with the aim of quantifying copper and iron contents in infant formula premixes (blends used in IF manufacturing which are designed to contain specified nutrients). The authors observed that PLS performances, especially with regard to validation, improved as the measuring depth increased. In the present study, this trend was also observed, however, finding an optimum at the third measurement depth. It is worth noting that depending on the laser energy and sample type, the optimum number of shots on the same location may change substantially since these parameters affect the laser-material interaction, for instance the size of the crater formed or the amount of ablated mass (Tognoni & Cristoforetti, 2016).

Table 2 also shows the performances for some of the PLS models developed with the accumulated spectra. In this regard, the modelling of accumulated spectra only proved to yield notable better performances for the first two laser shots as compared to applying PLS separately on these layers. A larger number of accumulations did not provide better models than using the third-layer-spectra alone. In several publications, authors chose to accumulate spectra as a means to mitigate signal fluctuations (Maria Markiewicz-Keszycka et al., 2017). The fact that, in this work, accumulating spectra did not considerably improved the results may be due to an already high sampling number (average of 100 locations) along with an optimum of 3 laser shots, the first two of which ablate away the surface which may have been contaminated.

Considering both pre-processing and sampling method, the best performing PLS model to predict sodium content was the third-layer spectra which had been normalised using the H I emission line at 656.29 nm.

3.3.2. Validation of the selected calibration model

The hydrogen-normalised third-layer-spectra model was used as the calibration to perform sodium content predictions. Fig. 2 (a) shows the values of RMSECV for each LV of this model. A number of 3 LVs was selected as further factors did not result in a notable improvement in terms of RMSECV while, at the same time, the quality of the predictions for the validation set decreased, indicating that a higher number of LVs could result in overfitting of the model. The first 3 main LVs explained approximately 95.7% of the total spectral variance.

Fig. 2 (b) shows the loading values for the first factor of the PLS model in the wavelength range assessed. One main sodium (Na I) emission line at 589.59 nm contributed to the loading values. Other Na I spectral lines were the doublet at 568.26 and 568.82 nm, and the emission line at 819.48 nm. These spectral lines had a relatively small contribution as compared to the sodium doublet at around 589 nm. Negative loading values were only observed for nitrogen (N I 744.23 and 746.83 nm) and oxygen (O I 777.19 nm), both elements showing minor values.

The PLS model exhibited an R^2 of 0.93 for the calibration. With regards to cross-validation, an R^2_{CV} value of 0.886 and an RMSECV of 0.373 mg/g were obtained, indicating a reasonable fit and accuracy of the calibration. The validation of the PLS model was carried out by predicting the Na contents of 2 samples not included in the training set with the aim of evaluating the robustness of the model. The model exhibited a good prediction accuracy as indicated by a high R^2_p (coefficient of determination for the validation set) of 0.967 and a RMSEP value of 0.129 mg Na/g. Fig. 3 shows the PLS calibration curve with the predicted values for the validation set. To further evaluate the closeness of the predictions to the actual values of concentration, the relative error (RE) was calculated as reported elsewhere (Câmara et al., 2017). The RE value of the validation set was 7.22%.

Additionally, Na contents for 2 follow-on formulas were also predicted in order to explore the model's response to different formulations of infant products. In this case, the predictions were not as accurate as the validation set, giving a RE value of 23.32%. However, this result may indicate that the model can provide reasonable predictions even with a certain degree of variability in the raw materials.

As mentioned before , the best performance was given by spectra collected after 3 laser shots. To further investigate why the third layer provided better results, sodium content was predicted, in this case, for each location in the 10×10 measuring grid. In order to do so, the raw spectral data acquired from sample V2, chosen as a point close to the centre of the calibration curve, was normalised by the hydrogen emission line without averaging the data of multiple locations, i.e. obtaining 500 pre-processed spectra instead of 5. Na contents were subsequently predicted employing the coefficients extracted from the PLS model. Fig. 4 shows a schematic representation of the V2 pellet displaying sodium content in each spatial position for the first 3 measurement depths. The same intensity scale for the three measurements was implemented to allow comparison. It can be observed that the predictions for the third layer, Fig.4(c), provided a more homogeneously distributed sodium within the analysed area.

The limit of detection of the model was estimated by following the pseudounivariate approach as described in Eq. 2. The LOD value corresponding to the calibration model was 1.11 mg/g.

4. Conclusions

LIBS was successfully applied for quantifying sodium over a range in conformity with the product's regulatory guidelines, hence, demonstrating the feasibility of the technique as a potential screening tool for IF manufacturing. Multivariate analysis with PLS was applied to spectral data processed by a range of different pre-processing techniques, measuring depths and accumulations. The resulting calibration models were compared in terms of PLS performance: coefficients of determination and root-mean-square errors; for calibration (R^2, RMSEC), leave-one-out cross-validation (R^2_{CV}, RMSECV) and validation (R^2_p, RMSEP). The best PLS calibration was obtained using the third-layer spectra normalised by the H I emission line at 656.29 nm, yielding a R^2 of 0.93 and a R^2_{CV} of 0.886. When performing validation of this model, the resulting R^2_p and RMSEP values were 0.967 and 0.129 mg Na/g respectively, proving its ability to accurately predict samples not included in the calibration set.

In this study, accumulation of the spectra on the same spot did not notably improve the performances of the PLS models as compared to using the third layer alone. Furthermore, chemical mapping with PLS of the analysed area (100 measurements in a 10×10 grid pattern) showed that sodium was more homogeneously distributed than for the first two layers. These results suggested that conditioning the surface of the pelletized sample, while keeping a low number of shots on the same spot, can provide a good predictive accuracy without the need of large sampling numbers.

Acknowledgements

Funding: The authors would like to acknowledge funding from the Food Institutional Research Measure, administered by the Department of Agriculture, Food and the Marine of Ireland (Grant agreement: 14/F/866).

References

Abdi, H. (2010). Partial least squares regression and projection on latent structure regression (PLS Regression). *Wiley Interdisciplinary Reviews: Computational Statistics*, *2*(1), 97–106. http://doi.org/10.1002/wics.51

Allegrini, F., & Olivieri, A. C. (2014). IUPAC-Consistent Approach to the Limit of Detection in Partial Least-Squares Calibration. *Analytical Chemistry*, *86*(15), 7858–7866.

http://doi.org/10.1021/ac501786u

Andersen, M.-B. S., Frydenvang, J., Henckel, P., & Rinnan, Å. (2016). The potential of laser-induced breakdown spectroscopy for industrial at-line monitoring of calcium content in comminuted poultry meat. *Food Control*, *64*, 226–233. http://doi.org/10.1016/j.foodcont.2016.01.001

Bilge, G., Sezer, B., Eseller, K. E., Berberoglu, H., Topcu, A., & Boyaci, I. H. (2016). Determination of whey adulteration in milk powder by using laser induced breakdown spectroscopy. *Food Chemistry*, *212*, 183–188. http://doi.org/10.1016/j.foodchem.2016.05.169

Blanchard, E., Zhu, P., & Schuck, P. (2013). Infant formula powders. In B. Bhandari, N. Bansal, M. Zhang, & P. Schuck (Eds.), *Handbook of Food Powders* (pp. 465–483). Cambridge, UK: Woodhead Publishing. http://doi.org/10.1533/9780857098672.3.465

Cama-Moncunill, R., Casado-Gavalda, M. P., Cama-Moncunill, X., Markiewicz-Keszycka, M., Dixit, Y., Cullen, P. J., & Sullivan, C. (2017). Quantification of trace metals in infant formula premixes using laser-induced breakdown spectroscopy. *Spectrochimica Acta Part B: Atomic Spectroscopy*, *135*, 6–14. http://doi.org/10.1016/j.sab.2017.06.014

Cama-Moncunill, X., Markiewicz-Keszycka, M., Dixit, Y., Cama-Moncunill, R., Casado-Gavalda, M. P., Cullen, P. J., & Sullivan, C. (2017). Feasibility of laser-induced breakdown spectroscopy (LIBS) as an at-line validation tool for calcium determination in infant formula. *Food Control*, *78*, 304–310. http://doi.org/10.1016/j.foodcont.2017.03.005

Câmara, A. B. F., de Carvalho, L. S., de Morais, C. L. M., de Lima, L. A. S., de Araújo, H. O. M., de Oliveira, F. M., & de Lima, K. M. G. (2017). MCR-ALS and PLS coupled to NIR/MIR spectroscopies for quantification and identification of adulterant in biodiesel-diesel blends. *Fuel*, *210*, 497–506. http://doi.org/10.1016/J.FUEL.2017.08.072

Campbell, K. J., Hendrie, G., Nowson, C., Grimes, C. A., Riley, M., Lioret, S., & McNaughton, S. A. (2014). Sources and Correlates of Sodium Consumption in the First 2 Years of Life. *Journal of the Academy of Nutrition and Dietetics*, *114*(10), 1525–1532.e2. http://doi.org/10.1016/j.jand.2014.04.028

Codex. (2007). *Standard for infant formula and formulas for special medical purposes intended for infants, CODEX STAN 72 – 1981*. Rome, Italy: FAO/WHO Codex Alimentarius.

Cremers, D. A., & Radziemski, L. J. (2013). *Handbook of Laser-Induced Breakdown Spectroscopy* (2nd ed.). Chichester, UK: John Wiley & Sons Ltd.

Cullen, P., Bakalis, S., & Sullivan, C. (2017). Advances in control of food mixing operations. *Current Opinion in Food Science*, *17*(Supplement C), 89–93. http://doi.org/https://doi.org/10.1016/j.cofs.2017.11.002

Dixit, Y., Casado-Gavalda, M. P., Cama-Moncunill, R., Cama-Moncunill, X., Markiewicz-Keszycka, M., Jacoby, F., … Sullivan, C. (2017). Introduction to laser induced breakdown spectroscopy imaging in food: Salt diffusion in meat. *Journal of Food Engineering*. http://doi.org/10.1016/j.jfoodeng.2017.08.010

dos Santos Augusto, A., Barsanelli, P. L., Pereira, F. M. V., & Pereira-Filho, E. R. (2017). Calibration strategies for the direct determination of Ca, K, and Mg in commercial samples of powdered milk and solid dietary supplements using laser-induced breakdown spectroscopy (LIBS). *Food Research International*. http://doi.org/10.1016/j.foodres.2017.01.027

El Haddad, J., Canioni, L., & Bousquet, B. (2014). Good practices in LIBS analysis: Review and advices. *Spectrochimica Acta Part B: Atomic Spectroscopy*, *101*, 171–182. http://doi.org/10.1016/j.sab.2014.08.039

Ferreira, E. C., Menezes, E. A., Matos, W. O., Milori, D. M. B. P., Nogueira, A. R. A., &

Martin-Neto, L. (2010). Determination of Ca in breakfast cereals by laser induced breakdown spectroscopy. *Food Control*, *21*(10), 1327–1330. http://doi.org/10.1016/j.foodcont.2010.04.004

Guo, M. (2014). 2 – Chemical composition of human milk. In M. Guo (Ed.), *Human Milk Biochemistry and Infant Formula Manufacturing Technology* (pp. 19–32). Cambridge, UK: Woodhead Publishing. http://doi.org/10.1533/9780857099150.1.19

Jantzi, S. C., Motto-Ros, V., Trichard, F., Markushin, Y., Melikechi, N., & De Giacomo, A. (2016). Sample treatment and preparation for laser-induced breakdown spectroscopy. *Spectrochimica Acta Part B: Atomic Spectroscopy*, *115*, 52–63. http://doi.org/10.1016/j.sab.2015.11.002

Jiang, Y. J. (2014). 11 – Infant formula product regulation. In M. Guo (Ed.), *Human Milk Biochemistry and Infant Formula Manufacturing Technology* (pp. 273–310). Cambridge, UK: Woodhead Publishing. http://doi.org/10.1533/9780857099150.3.273

John, K. A., Cogswell, M. E., Zhao, L., Maalouf, J., Gunn, J. P., & Merritt, R. K. (2016). US consumer attitudes toward sodium in baby and toddler foods. *Appetite*, *103*, 171–175. http://doi.org/10.1016/J.APPET.2016.04.009

Kim, G., Kwak, J., Choi, J., & Park, K. (2012). Detection of Nutrient Elements and Contamination by Pesticides in Spinach and Rice Samples Using Laser-Induced Breakdown Spectroscopy (LIBS). *Journal of Agricultural and Food Chemistry*, *60*(3), 718–724. http://doi.org/10.1021/jf203518f

Kramida, A., Ralchenko, Y., Reader, J., & NIST ASD team. (2016). NIST Atomic Spectra Database (version 5.4). Retrieved December 4, 2017, from https://www.nist.gov/pml/atomic-spectra-database

Lei, W. Q., El Haddad, J., Motto-Ros, V., Gilon-Delepine, N., Stankova, A., Ma, Q. L., … Yu, J. (2011). Comparative measurements of mineral elements in milk powders with laser-induced breakdown spectroscopy and inductively coupled plasma atomic emission spectroscopy. *Analytical and Bioanalytical Chemistry*, *400*(10), 3303–3313. http://doi.org/10.1007/s00216-011-4813-x

Markiewicz-Keszycka, M., Cama-Moncunill, X., Casado-Gavalda, M. P., Dixit, Y., Cama-Moncunill, R., Cullen, P. J., & Sullivan, C. (2017). Laser-induced breakdown spectroscopy (LIBS) for food analysis: A review. *Trends in Food Science & Technology*, *65*, 80–93. http://doi.org/10.1016/j.tifs.2017.05.005

Markiewicz-Keszycka, M., Casado-Gavalda, M. P., Cama-Moncunill, X., Cama-Moncunill, R., Dixit, Y., Cullen, P. J., & Sullivan, C. (2018). Laser-induced breakdown spectroscopy (LIBS) for rapid analysis of ash, potassium and magnesium in gluten free flours. *Food Chemistry*, *244*. http://doi.org/10.1016/j.foodchem.2017.10.063

Masotti, F., Erba, D., De Noni, I., & Pellegrino, L. (2012). Rapid determination of sodium in milk and milk products by capillary zone electrophoresis. *Journal of Dairy Science*, *95*(6), 2872–2881. http://doi.org/10.3168/JDS.2011-5146

Mevik, B.-H., Wehrens, R., & Liland, K. H. (2015). *Pls: Partial Least Squares and Principal Component Regression*. Retrieved from https://cran.r-project.org/web/packages/pls/index.html

Misra, N. N., Sullivan, C., & Cullen, P. J. (2015). Process Analytical Technology (PAT) and Multivariate Methods for Downstream Processes. *Current Biochemical Engineering*, *2*(1), 4–16. http://doi.org/10.2174/2213385203666150219231836

Moncayo, S., Manzoor, S., Rosales, J. D., Anzano, J., & Caceres, J. O. (2017). Qualitative and quantitative analysis of milk for the detection of adulteration by Laser Induced Breakdown Spectroscopy (LIBS). *Food Chemistry*, *232*, 322–328. http://doi.org/10.1016/j.foodchem.2017.04.017

Montagne, D.-H., Van Dael, P., Skanderby, M., & Hugelshofer, W. (2009). 9 – Infant

Formulae – Powders and Liquids. In A. Y. Tamime (Ed.), *Dairy Powders and Concentrated Products* (pp. 294–331). Oxford, UK: Blackwell Publishing.

Poitevin, E. (2016). Official Methods for the Determination of Minerals and Trace Elements in Infant Formula and Milk Products: A Review. *Journal of AOAC International*. Retrieved from http://www.ingentaconnect.com/content/aoac/jaoac/2016/00000099/00000001/art00009

R Core Team. (2014). *R: A language and environment for statistical computing*. Viena, Austria. Retrieved from http://www.r-poject.org/

Sezer, B., Bilge, G., & Boyaci, I. H. (2017). Capabilities and limitations of LIBS in food analysis. *TrAC Trends in Analytical Chemistry*, *97*(Supplement C), 345–353. http://doi.org/https://doi.org/10.1016/j.trac.2017.10.003

Sobron, P., Wang, A., & Sobron, F. (2012). Extraction of compositional and hydration information of sulfates from laser-induced plasma spectra recorded under Mars atmospheric conditions — Implications for ChemCam investigations on Curiosity rover. *Spectrochimica Acta Part B: Atomic Spectroscopy*, *68*, 1–16. http://doi.org/https://doi.org/10.1016/j.sab.2012.01.002

Tamm, A., Bolumar, T., Bajovic, B., & Toepfl, S. (2016). Salt (NaCl) reduction in cooked ham by a combined approach of high pressure treatment and the salt replacer KCl. *Innovative Food Science & Emerging Technologies*, *36*(Supplement C), 294–302. http://doi.org/https://doi.org/10.1016/j.ifset.2016.07.010

Tognoni, E., & Cristoforetti, G. (2016). Signal and noise in Laser Induced Breakdown Spectroscopy: An introductory review. *Optics & Laser Technology*, *79*, 164–172. http://doi.org/10.1016/j.optlastec.2015.12.010

van den Berg, F., Lyndgaard, C. B., Sørensen, K. M., & Engelsen, S. B. (2013). Process Analytical Technology in the food industry. *Trends in Food Science & Technology*, *31*(1), 27–35. http://doi.org/10.1016/j.tifs.2012.04.007

Wu, D., & Sun, D.-W. (2013). Advanced applications of hyperspectral imaging technology for food quality and safety analysis and assessment: A review — Part I: Fundamentals. *Innovative Food Science & Emerging Technologies*, *19*, 1–14. http://doi.org/10.1016/J.IFSET.2013.04.014

Table 1

Sodium contents in milligrams per gram of samples corresponding to calibration (C1–C5) and validation (V1–V4) determined by AAS.

Sample	Constituents	Batch 1	Batch 2	Extra validation
		Na content (mg/g) [a]	Na content (mg/g) [a]	Na content (mg/g) [a]
C1	IF + lactose	0.48 ± 0.05	0.54 ± 0.03	–
C2	IF	1.40 ± 0.21	1.34 ± 0.07	–
C3	IF + NaCl	2.11 ± 0.11	2.07 ± 0.02	–
C4	IF + NaCl	2.78 ± 0.16	2.72 ± 0.07	–
C5	IF + NaCl	3.69 ± 0.54	3.74 ± 0.18	–
V1	IF + lactose	0.93 ± 0.06	0.98 ± 0.06	–
V2	IF + NaCl	2.22 ± 0.04	2.48 ± 0.21	–
V3	follow-on	–	–	1.18 ± 0.04
V4	follow-on	–	–	2.38 ± 0.36

[a] Contents expressed as mean ± standard deviation of three replicates.

Table 2

Summary of performances for the PLS models developed using different sampling methods and pre-processing techniques.

Experiment	Depth	Pre-processing	Calibration			Cross-validation		Validation	
			LVs	R^2	RMSEC	R^2_{CV}	RMSECV	R^2_p	RMSEP
Single layer	3	None	3	0.851	0.426	0.771	0.529	0.904	0.218
Single layer	1	H I 656.3	3	0.899	0.352	0.822	0.465	0.612	0.438
Single layer	2	H I 656.3	3	0.856	0.419	0.776	0.523	0.498	0.498
Single layer	3	H I 656.3	3	0.930	0.291	0.886	0.373	0.967	0.129
Single layer	4	H I 656.3	3	0.879	0.384	0.786	0.511	0.915	0.205
Single layer	5	H I 656.3	3	0.824	0.463	0.665	0.639	0.914	0.207
Accumulations	4 (0[a]/4[b])	H I 656.3	3	0.931	0.290	0.884	0.377	0.914	0.206
Accumulations	5 (0[a]/5[b])	H I 656.3	3	0.916	0.320	0.856	0.419	0.935	0.179
Accumulations	4 (1[a]/3[b])	H I 656.3	3	0.924	0.287	0.872	0.366	0.940	0.213
Single layer	3	Ca I 422.6	3	0.937	0.276	0.893	0.361	0.966	0.131
Single layer	3	C I 247.9	3	0.923	0.306	0.876	0.389	0.894	0.229
Single layer	3	K I 766.4	3	0.942	0.266	0.911	0.330	0.908	0.213
Single layer	3	SNV	3	0.938	0.276	0.888	0.369	0.945	0.164
Single layer	4	SNV	3	0.917	0.318	0.851	0.426	0.866	0.258
Single layer	5	SNV	2	0.865	0.405	0.816	0.473	0.911	0.210
Accumulations	4 (0[a]/4[b])	SNV	2	0.879	0.384	0.840	0.442	0.849	0.274
Accumulations	5 (0[a]/5[b])	SNV	2	0.881	0.382	0.841	0.441	0.897	0.225
Accumulations	4 (1[a]/3[b])	SNV	2	0.878	0.389	0.831	0.446	0.888	0.312
Single layer	3	Euclidean	3	0.938	0.274	0.889	0.367	0.950	0.157
Single layer	4	Euclidean	2	0.871	0.397	0.824	0.463	0.889	0.234
Single layer	5	Euclidean	2	0.865	0.405	0.816	0.474	0.910	0.211
Accumulations	4	Euclidean	2	0.879	0.383	0.839	0.443	0.811	0.306
Accumulations	5	Euclidean	2	0.881	0.381	0.841	0.441	0.874	0.250

[a] Number of conditioning shots.

[b] Number of accumulated spectra.

Figure 1

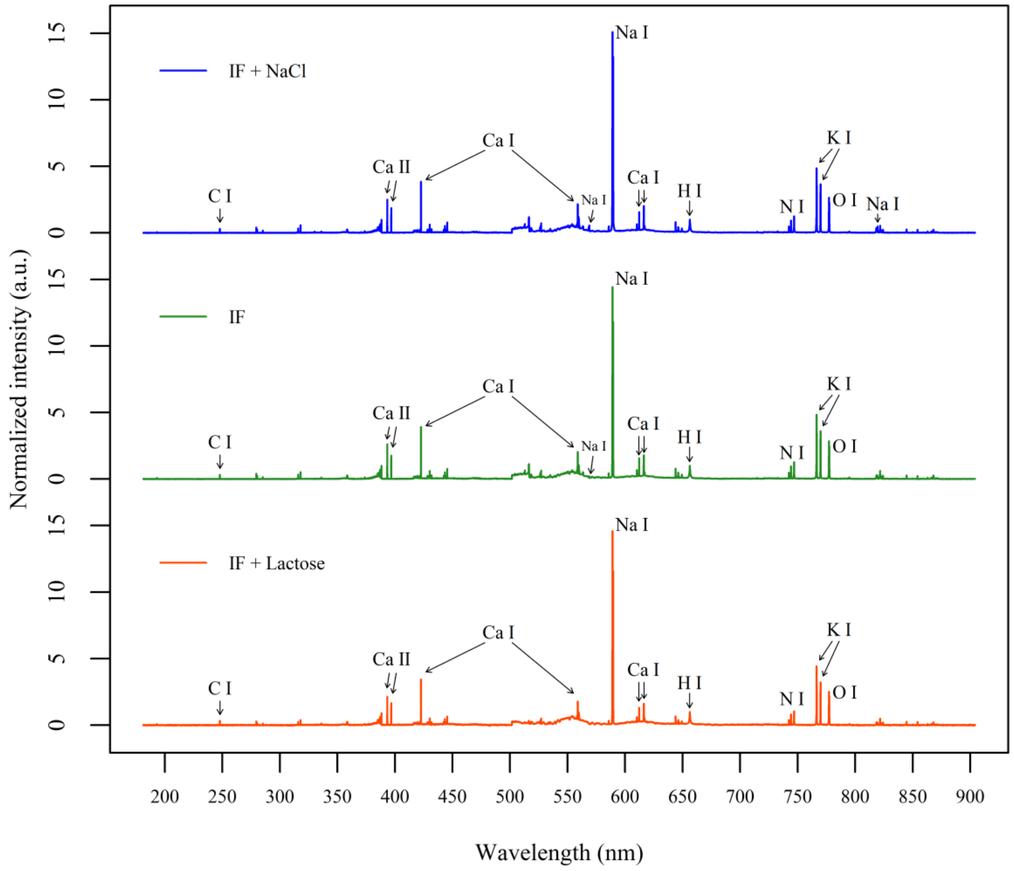

Fig. 1. Averaged spectra corresponding to, from top to bottom, the sodium chloride -IF mixture at approx. 3.7 mg Na/g, the pure IF sample at approx. 1.3 mg Na/g and the sodium lactose-IF mixture at approx. 0.5 mg Na/g. Spectra are vertically offset for illustration purposes.

Figure 2

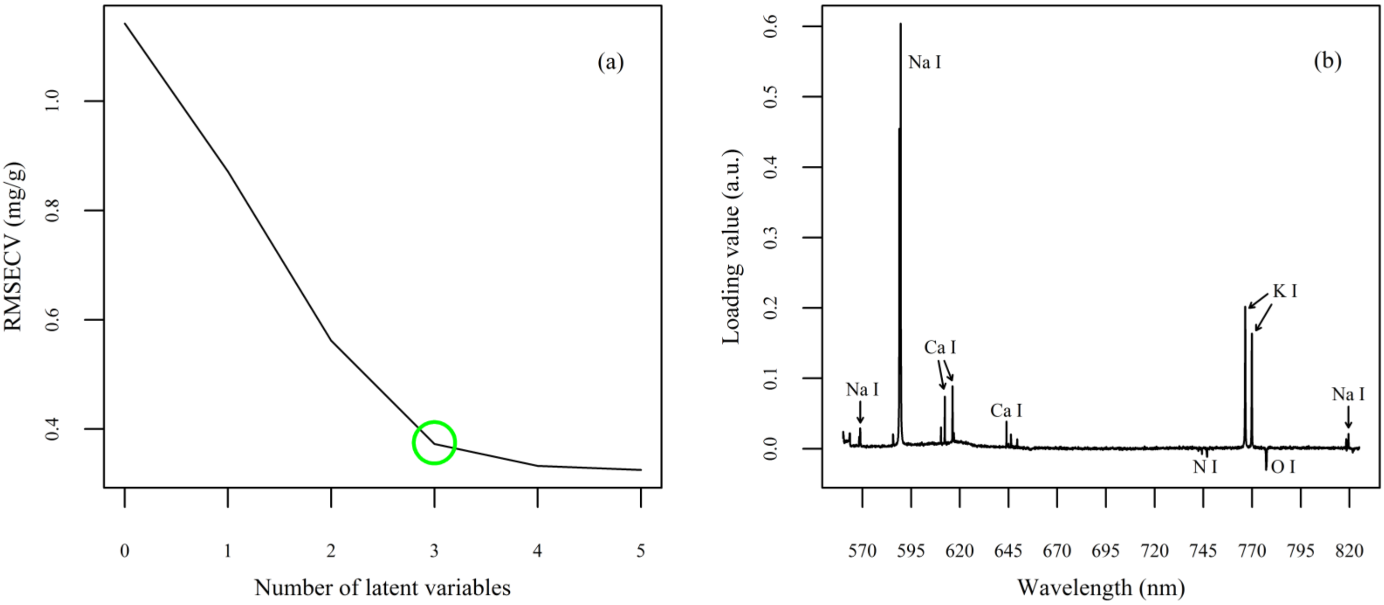

Fig. 2. (a) RMSECV (root-mean-square error of cross-validation) for each number of PLS factors or latent variables. (b) Loading values of each wavelength for the first latent variable.

Figure 3

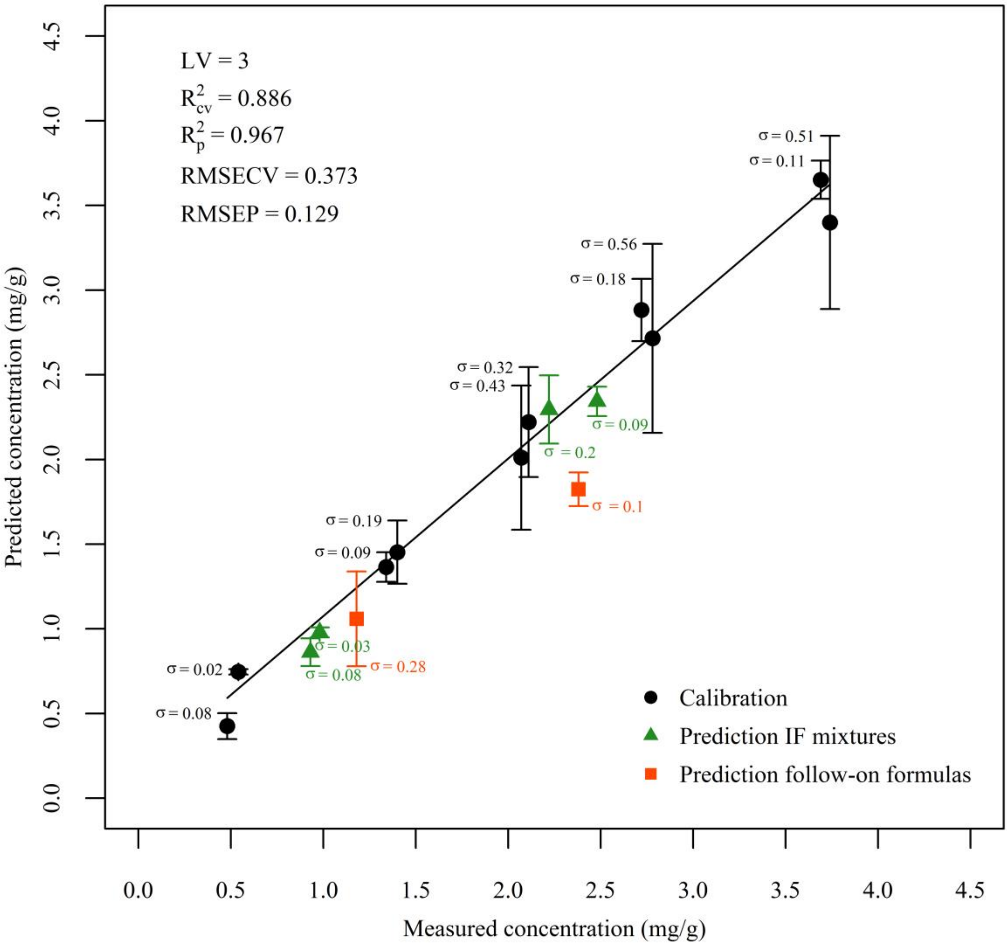

Fig. 3. PLS calibration model developed using the third-layer spectra and normalised by the H I 656.29 emission line showing predicted Na contents for the validation and follow-on formulas sets. Standard deviation values (σ) are expressed in mg/g.

Figure 4

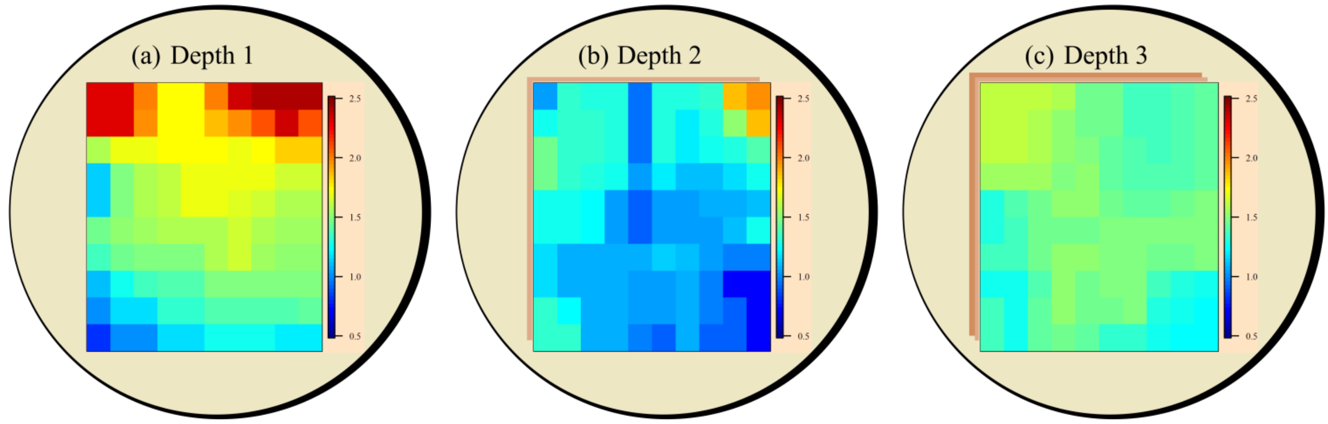

Fig.4. Predicted sodium maps for the validation sample at 2.48 mg/g of sodium for the first three depths: (a) first layer, (b) second layer, (c) third layer. The same intensity scale was implemented for the three samples to facilitate comparison.